universe

MDPI

Article

The Macro-Physics of the Quark-Nova: Astrophysical Implications

Rachid Ouyed

Department of Physics and Astronomy, The University of Calgary, Calgary, AB T2N 1N4, Canada; rouyed@ucalgary.ca

Abstract: A quark-nova is a hypothetical stellar evolution branch where a neutron star converts explosively into a quark star. Here, we discuss the intimate coupling between the micro-physics and macro-physics of the quark-nova and provide a prescription for how to couple the Burn-UD code to the stellar evolution code in order to simulate neutron-star-to-quark-star burning at stellar scales and estimate the resulting energy release and ejecta. Once formed, the thermal evolution of the proto-quark star follows. We found much higher peak neutrino luminosities (>10^{55} erg/s) and a higher energy neutrino (i.e., harder) spectrum than previous stellar evolution studies of proto-neutron stars. We derived the neutrino counts that observatories such as Super-Kamiokande-III and Halo-II should expect and suggest how these can differentiate between a supernova and a quark-nova. Due to the high peak neutrino luminosities, neutrino pair annihilation can deposit as much as 10^{52} ergs in kinetic energy in the matter overlaying the neutrinosphere, yielding relativistic quark-nova ejecta. We show how the quark-nova could help us understand many still enigmatic high-energy astrophysical transients, such as super-luminous supernovae, gamma-ray bursts and fast radio bursts.

Keywords: neutron stars; nuclear matter aspects; quark deconfinement; quark-gluon plasma production; phase-transition

Citation: Ouyed, R. The Macro-Physics of the Quark-Nova: Astrophysical Implications. *Universe* **2022**, *8*, 322. https://doi.org/10.3390/universe8060322

Academic Editors: Veronica Dexheimer and Rodrigo Negreiros

Received: 21 March 2022
Accepted: 30 May 2022
Published: 9 June 2022

Publisher's Note: MDPI stays neutral with regard to jurisdictional claims in published maps and institutional affiliations.

1. Introduction

1.1. The Energetic Problem in Astrophysics

High-energy astrophysics suffers from an energy problem. The total integrated luminosity observed in the universe cannot be completely accounted for by existing theoretical models. In almost all astrophysical explosive events that generate 10^{53} ergs or more in kinetic energy and radiation, the engine remains elusive. For example, the energies observed in core-collapse supernovae [1] or gamma-ray bursts cannot be reproduced consistently with computer simulations [2]. Specifically, in the case of core-collapse supernovae, computer simulations cannot form robust explosions from first principles for all the relevant progenitor masses [1]. In the case of even more energetic phenomena, such as superluminous supernova, that have kinetic energies of around 10^{52} ergs, the engine remains even more elusive. Similar issues appear with gamma-ray bursts, which suffer from related energy budget problems. Recently, the associated gamma-ray burst observation of the gravitational wave [3] of a neutron star merger showed the same energy budget problems, where the observed luminosity was much milder than for other known GRBs. These anomalies suggest the need for a novel source that can "balance" this budget problem and can be accounted for by the physics required to fix it.

There are various observational phenomena that indicate the explosion of a neutron star. For example, most models that seek to explain the large luminosities and kinetic energy of super-luminous supernovae do so by using a "point source" that injects energy into an envelope of (1–20) $M_{\odot}$, whether this point source is a core-collapse supernova, or a magnetar [4]. However, in the case of transforming a core-collapse supernova's energy into luminosity by shocking it with a 1 $M_{\odot}$ envelope or "wall", it is necessary to explain the source of the envelope itself, which is a non-trivial problem. In the case of a magnetar, it is necessary to assume almost 100 percent efficiency of conversion between the rotational

energy and the luminosity/kinetic energy of the envelope [4]. Furthermore, it is necessary to explain the source of the large magnetic field.

1.2. Exploding Neutron Stars?

We argue that this points to the explosive transition (i.e., combustion) of a neutron star to a quark star. In the canonical case, a neutron-star is the final evolutionary path of massive (>8 $M_{\odot}$) stars which are the remnants of a core-collapse supernova explosion. However, we propose a further evolutionary stage for some of these neutron stars, that is, their explosive collapse into a more compact configuration—the quark star. We refer to this "explosion pathway" as a quark-nova [5]. The energy released in the explosion is a combination of the gravitational binding energy during the neutron star's core-collapse and the nuclear binding energy released from the neutron matter decaying to more stable quark matter made of up, down and strange quarks (hereafter *(u,d,s)*). The model makes use of the Bodmer–Witten–Terazawa hypothesis (BWTH; [6–8]), which argues that *(u,d,s)*, not baryonic matter, is the most stable form of matter in the universe. The Quark-Nova group have developed this model theoretically and primarily numerically (by developing the Burn-UD code) over many years, starting with their pioneering paper of 2002 [5].

If *(u,d,s)* quark-matter is the most stable form of matter in the universe, then it follows that neutron stars may decay into more stable quark stars through an exothermic process. According to the BWT hypothesis, the reason why hadronic matter does not spontaneously decay into *(u,d,s)* matter is that there is an intermediate higher energy state of *(u,d)* matter. To diminish this energy barrier, there need to be sufficient s-quarks available to trigger the combustion process. Another way of stating this, is that s-quarks act as catalysts that lower the free energy barrier, allowing hadronic matter to decay into a lower state of *(u,d,s)* matter. This energy barrier could explain why *(u,d,s)* matter is much scarcer than hadronic matter to the extent that we have not detected the former. In other words, although empirically we do not find two-flavour-quark matter at zero pressure, the addition of an extra degree of freedom, such as strange quarks, could decrease the Fermi energy for the same baryon number density, lowering the quark matter's free energy below the free energies of both hadronic and two-flavoured quark matter.

Since this hypothesis was proposed, many interesting scenarios have been postulated in both astrophysics and particle physics. For example, the existence of pure strange quark stars, and fragments of *(u,d,s)* matter, called strangelets, have been suggested. Beyond the existence of macroscopic objects, such as strange quark stars, another interesting consequence of the BWTH is the release of large amounts of energy when hadronic matter converts to *(u,d,s)* matter. Assuming a bag constant of $B = 145$ MeV, using the above model, the energy per baryon becomes ∼840 MeV which is roughly 100 MeV less than for ordinary hadronic matter (∼930 MeV) [9]. This implies that a conversion from hadronic to *(u,d,s)* matter should release about 100 MeV per converted baryon. Assuming a neutron star has about 10^{57} baryons, conversion of every baryon into *(u,d,s)* matter would generate $\sim 10^{53}$ ergs in total energy. While this is of the same order of magnitude for typical explosive events in astrophysics, such as core-collapse supernovae, the energy is hardly harnessed since it is emitted as neutrinos. The advent of the quark-nova allowed novel channels which would convert this energy to photon fireballs and to the kinetic energy of the quark-nova ejecta which can be easily harnessed with revolutionary consequences for high-energy astrophysics. We discuss how it can be harnessed in a newly born neutron star (i.e., embedded deep within its supernova ejecta) or in an old one (in isolation). This contribution focuses on the macro-physics of the neutron-star-to-quark star conversion in order to understand the unique features of quark-nova dynamics and energetics at stellar scales. We refer the reader to a complementary paper [10] where we discuss in detail the micro-physics of the *hadron*-to-*(u,d,s)* conversion which is briefly reviewed here in Section 1.4. Firstly, however, we remind the reader of strategies described in the literature when exploring the transition. In particular, we explain why the correct choice for the thermodynamic potential in a transition which is not in mechanical equilibrium (as in the

quark-nova scenario) is the Helmholtz potential, rather than the Gibbs potential which is usually cited in the literature.

1.3. The Hadron-Quark Transition: The Thermodynamics

Glendenning [11] pointed out that, in complex systems of more than one conserved charge, the system does not need to be locally electrically neutral, only globally so. This allows for a complex mixed phase to exist during the transition of nuclear to quark matter where various charges, including baryon number, electric charge, and quark flavors, are conserved. This led to a rich literature exploring the hadron-to-quark matter transition which can be divided into three main streams including smooth (i.e., cross-over), Gibbs (i.e., soft) and Maxwell (i.e., sharp first-order) transitions. The nature of the transition depends strongly on the EoS of the hadronic and quark matter. In the Maxwell construction, the nuclear-quark phase transition is first-order (e.g., [12–15] and references therein) and the imposition of local charge neutrality would lead to a sharp interface (because of the high surface tension) with a width in the order of femtometers (for details see [11,16–18]). This is in contrast to a Gibbs construction where there is a mixed region where hadron matter and quark matter coexist [19–24]. In the case of a smooth cross-over, interpolation procedures are used to connect the two phases (e.g., [25,26] and references therein). The Gibbs construction also appeals to a smooth transition into the mixed phase but the fraction of each phase is determined self-consistently and is independent of the interpolation method adopted. For completeness, we mention other examples of a smooth cross-over transition, such as the chiral model [27] and the quarkyonic model [28]. A quark phase with additional hadronic admixtures, such as hyperons and meson condensates, has also been explored in early work [29].

The Gibbs potential is typically chosen to model most phase transitions since the timescales are usually large enough that the sound waves flatten any pressure spatial gradient across the interface. The Gibbs potential is generally deployed in many studies of phases of matter inside compact stars, since the objects of study are in a steady state, sufficient time has passed so that the phases are in mechanical equilibrium, and the variables that are being studied, such as the radius and mass, are steady-state, time-independent values. Yet, not all phase transitions are in mechanical equilibrium. If the timescales are short enough so that sound waves have not flattened the pressure gradients, then the Gibbs potential becomes inaccurate. The correct choice for the thermodynamic potential to represent the free energy depends on which thermodynamic quantities are approximated as constant when a system changes its thermodynamic state. If it is assumed that the pressure P and the temperature T remain constant through the change (i.e., $dP = dT = 0$), then the decrease in free energy $dG \leq 0$ is equivalent to the second law; that is, the increase in entropy $dS \geq 0$. In the case of the Helmholtz energy, $dF \leq 0$ is equivalent to $dS \geq 0$ if $dV = 0$ (where V is the volume) and $dT = 0$. This difference between the Gibbs and Helmholtz potential is crucial in the context of hadron-quark phase transitions (see discussion in [10]).

In our case, the first-order phase transition of nuclear to quark matter conserves various charges, including baryon number, electric charge, and quark flavors. The fact that the system does not have to be locally neutral gives rise to a complex mixed phase made of differently shaped bubbles of quark matter embedded in hadronic matter. We find that the correct choice for the thermodynamic potential is the Helmholtz potential, which contrasts with the usual Gibbs potential found in the literature. To justify the use of the Helmholtz instead of the Gibbs potential, we note that the most relevant (i.e., the largest) timescale in our approach to the hadron-quark matter phase transition is the weak interaction timescale which is of the order of 10^{-8} s; the timescale of energy release due to quark beta equilibration is also relevant. Our study must also resolve the sonic timescales which are of the order of 10^{-11} s, as the pressure gradients are dynamically important. Since the sonic time is twelve orders of magnitude larger than the strong interaction ($\sim 10^{-23}$ s), a study that resolves the sonic time cannot assume the interface is

in mechanical equilibrium—in other words, that $dP = 0$. In the case of the hadron-quark phase transition, the strong interaction acts at a timescale of $\sim 10^{-23}$ s, which is much faster than the hydrodynamics that may flatten the pressure gradient. Therefore, we must choose the Helmholtz thermodynamic potential over the Gibbs one. In other words, hadronic matter will convert to quark matter if the Helmholtz free energy is lower for quark matter than for hadronic matter, a point discussed in detail in Section 2.2 in [10] (and references therein).

1.4. Quark-Nova: A Brief Review of the Microphysics

The mechanism of the quark-nova is intimately linked to the strong force which governs the interaction between quarks and also gives rise to the nuclear force. In astrophysics, quantum chromodynamics (QCD) becomes relevant in the context of compact objects. This is because the cores of compact objects are so dense that they become thermodynamically ideal sites for the phase-transition of hadronic to quark matter.

Quark deconfinement appears at extremely high temperatures or densities. This is due to the property of asymptotic freedom where the high momentum exchange between quarks weakens the attractive interaction between them. So, for the "quarks" to be released/deconfined, they need to collide with extreme momenta. Since temperature is a measure of kinetic energies, high temperatures are a way to trigger this deconfinement. In the case of high densities, fermions, such as quarks, are compressed into having high Fermi energies, triggering high momentum exchange.

In Earth-based experiments, particle accelerators tap into the high temperature regime by triggering very high energy collisions. However quark deconfinement in compact stars cannot be probed through experiments, since deconfinement appears at low temperatures but high ($\sim 10^{15}$ g cm^{-3}) densities. This give rise to the need to use compact star observations to probe the QCD phase diagram. The existence of exotic particles in the core of compact stars is, therefore, an ideal laboratory for the study of exotic particles. Given the high Fermi energies, and, therefore, high momentum exchanges in the cores of compact stars, nucleation of quark matter inside them can be expected.

The BWTH hypothesis referred to previously states that matter with the lowest binding energy could be *(u,d,s)* quark matter. The main reason for this is that the existence of a third degree of freedom in the form of s-quarks in general lowers the Fermi energy of the matter. In the MIT bag model, a simple approximation is that quark matter is in the form of a Fermi gas with a constant B that acts as the confinement pressure. A range of bag constants can be found where *(u,d,s)* quark matter is lower than the hadronic binding energy of $\sim$930 MeV, but, at the same time, where *(u,d)* matter has a higher binding energy than hadronic matter. This hypothesis therefore implies that macroscopic objects made of *(u,d,s)* matter are thermodynamically plausible.

The conversion of hadronic to quark matter could occur in the following way: Once two-flavoured quark matter is nucleated in the core of neutron stars, the weak interaction can turn some of the d quarks into s-quarks, lowering the Fermi energy of the quark matter. Because, at this point, the free energy of *(u,d,s)* matter is lower than the free energy of hadrons, the hadrons accreted by the quark core would find it energetically favourable to deconfine into lower energy quark matter. Eventually, the quark core would grow, engulfing the whole compact star, turning it into a pure *(u,d,s)* star. There are alternate scenarios for conversion of a whole compact star to a *(u,d,s)* star including, for example, through "seeding" of cosmic strangelets (e.g., [30]), or dark-matter annihilation in neutron stars heating up parcels of neutron star matter making conditions favorable for the creation of quark bubbles [31].

Although the 10^{53} ergs of energy release predicted by energetics compares favorably to explosive events such as supernovae, whether this energy is released explosively or in a slow simmer is not defined. Since the 1980s, different groups have sought to elucidate the phenomenology of this energy release. Olinto [30] pioneered a hydrodynamic formalism for exploring the conversion of hadronic to *(u,d,s)* quark matter as a hydrodynamic combustion

process. The conversion was modeled as a "combustion front" that "burns" hadronic fuel into *(u,d,s)* ash. However, the exact equations that govern this reaction zone, the reaction-diffusion-advection equations, cannot be solved in analytic form since they are non-linear. Olinto therefore needed to linearize the equations and impose mechanical equilibrium and derive semi-analytic, steady-state solutions. The study yielded timescales of conversion of minutes to days for the whole compact star, which would imply a slow simmer, since the timescale of a supernova explosion is about one second.

Another pioneering paper was published by Benvenuto et al. [32] in the late 1980s. In contrast to Olinto, the authors assumed an initial shock and solved the relativistic jump conditions. The model proposed leads to a steady-state solution but without the mechanical equilibrium assumed by Olinto. The approach yields a supersonic detonation, which Benvenuto et al. argue can provide enough kinetic energy to make a core-collapse supernova explode. Although this explosive solution contrasts with Olinto's much slower timescales, the reason is that a shock is assumed on an a priori basis, with arguments presented that the initial deconfined bubble of quark matter creates a sharp pressure discontinuity. Drago et al. [33] also solved the jump conditions without assuming mechanical equilibrium, but in their case they found that the combustion takes the form of subsonic deflagration.

All the literature on hadron-quark combustion before the 2010s can be roughly categorized as following either a mechanical equilibrium approach [30] or a jump condition approach [33], and has always assumed a steady state. Because of the variety of the assumptions made, such as whether a pressure equilibrium is assumed or not, or whether a shock is hypothesized as an initial condition or not, the timescales of conversion predicted for the compact star have varied by various orders of magnitude, from milliseconds to days.

1.5. The Burn-UD Code and Non-Premixed Combustion

Previous literature on this topic has reported very different results on the transition speed and energy as a consequence of incorrectly assuming premixed combustion (see discussion on this in [34]). However, the *(u,d*-to-*(u,d,s)* combustion is of the non-premixed type, a distinction that is critically important. In a hadron-quark combustion flame, the thermal conductivity plays a negligible role, since the activation occurs through the s-quark fraction, because it is ultimately the quantity of s-quarks in the quark phase that determines whether the quark matter has a lower free energy than the hadronic matter. A minimal amount of s-quarks in the NS core is sufficient to create "oxidation" (to represent it in chemical activation terminology). In traditional pre-mixed combustion, the oxidant must be mixed with the fuel so that, once the activation temperature is achieved, the fuel is burned. Some fuels come premixed with the oxidant, and, therefore, the combustion is fundamentally mediated by thermal conductivity. In our case, as the fuel and oxidant are not mixed, the transport of oxidants into the fuel becomes an important process, alongside the thermal conductivity. Since the s-quarks can be thought of as related to the activation temperature and as an oxidant, a proper treatment of the hadron-quark combustion process should be studied as a diffusion flame. Equally important, and unlike previous work, we include neutrinos which carry a non-negligible energy (in the hadron-quark combustion system, mass and energy are interchangeable) and momentum. We found a much more complex interplay between fluid dynamics and radiation which makes it impossible to compare our work to past investigations. Ultimately, it is the transport of s-quarks, in concert with neutrino transport and leptonic dynamics, that decides the behavior of the flame, which is very different from the way thermal conductivity acts in Arrhenius-type reactions. Thus, fundamentally, the non-premised scenario in the quark-nova model is different from that of past work (see in-depth analysis and discussion in [35,36]).

A hydrodynamic combustion code (the Burn-UD code; [35,36]) was developed by the Quark-Nova group to model in detail the non-premixed phase transition of hadronic to quark matter. The Burn-UD code allows the adoption of the Helmholtz, instead of the Gibbs, potential (see Section 1.3) and self-consistently couples the thermodynamics to the hydrodynamics, which is of crucial importance. It can be shown that this coupling allows

for a more rigorous capture of the propagation of the burning front with implications for the energetics in the case of a burning neutron star. For example, if the propagation of the burning front is too slow, the energy released is not efficiently transformed into kinetic energy, with the energy simply leaking out slowly as transparent neutrinos. The Burn-UD code consistently calculates how the weak interaction gives rise to particle and temperature spatial gradients that, in turn, trigger pressure gradients. A pressure gradient acts as a source of momentum density in the fluid, transforming some of the energy released into mechanical energy. The inclusion of the Helmholtz thermodynamic potential was found to lead to much larger neutrino luminosities (about two orders of magnitude larger than for the Gibbs potential) and larger burning speeds. Furthermore, the Helmholtz approach offers advantages numerically since it can borrow from the Gibbs construction, which avoids sharp density gradients in numerical experiments by employing a mixed phase (see Section 2.2 in [10]).

The Burn-UD code models the flame micro-physics for different equations of state (EOS) on both sides of the interface, i.e., for both the ash (up-down-strange quark phase) and the fuel (up-down quark phase). It also allows the user to explore strange-quark seeding produced by different processes. It is an *advection-reaction-diffusion* code which is essential for a proper treatment of the micro-physics of a burning front. Furthermore, having a precise understanding of the phase transition dynamics for different EOSs further aids in constraining the nature of the non-perturbative regimes of QCD in general (see Section 4.1). The Burn-UD code has evolved into a platform/software which can be used and shared by the QCD community exploring the phases of quark matter and by astrophysicists working on compact stars. The code provides a unique physical window to diagnose whether the combustion process will simmer quietly and slowly, lead to a transition from deflagration to detonation, or entail a (quark) core-collapse explosion.

Niebergal et al. [37], for the first time, in 2010 published a study that numerically solved the reaction-diffusion-advection equations for hadron-quark combustion. This study combined transport, chemical, and entropic processes into a numerical simulation. Not only was the burning velocity much faster than many of the previous estimates, but Niebergal et al. sugested that leptons may trigger feedback that can accelerate the burning front into supersonic detonation or quench it. Their argument was based on solving the jump conditions and parameterizing the cooling behind the front.

Later, Ouyed et al. [38] solved the reaction-diffusion-advection equations and coupled them to neutrino transport using a flux-limited diffusion scheme, and added an electron EOS and a hadronic matter (HM) EOS. Ouyed et al. confirmed numerically that leptons can trigger extreme feedbacks, with the burning halting completely for certain choices of the initial conditions. Ouyed et al.'s study was important in that it showed that, due to non-linear couplings between lepton physics and hydrodynamics, the simulation was extremely sensitive to the details of neutrino transport. This indicated that the system is genuinely a non-linear, dynamic process, and that simplifying it by imposing mechanical equilibrium or steady-state conditions was extremely inaccurate.

There are multiple ways that a quark-nova could be triggered. There are two "mechanisms" for initiating the combustion of a neutron star into a quark star. One mechanism relates to the core of a neutron star in some way reaching sufficiently high densities that favour the deconfinement of quark matter. These nucleated *(u,d)* quark bubbles, in turn, would beta equilibrate into *(u,d,s)* matter, and then, in accordance with the BWTH, grow, engulfing the whole neutron star [39]. However, the density at which quark matter deconfines is very uncertain. It could be that most neutron stars achieve the deconfinement density and, therefore, turn into quark stars. However if the deconfinement density is higher than that of the average core of a neutron star, then sufficiently high density could be achieved through other processes, such as accretion, fall-back from supernovae, or spin-down evolution, leading to a two-family compact star scenario, where quark stars and neutron stars coexist [40].

The other mechanism for triggering a quark-nova could be through "seeding". According to the BWTH, a strangelet that interacts with hadronic matter can convert the latter, provided that there is not an electrostatic barrier preventing the interaction. Since neutrons do not have a charge, neutron stars are an ideal site for strangelet contamination. The source of strangelets can be arbitrary; for example, cosmic strangelets can be released by a *(u,d,s)* star merger, or stranglets may be formed through the annihilation of dark matter in the core of neutron stars.

In summary, the quark-nova hypothesis (and the underlying microphysics) implies that the traditional picture of stellar evolution is not the whole story. There is the possibility that the neutron star would experience further collapse into a *(u,d,s)* star. Such a phenomenon would have similar dynamics and energetics as a core-collapse supernova, with approximately $\sim 10^{53}$ ergs released of both chemical and gravitational binding energy. Such an addition to the stellar evolution picture has immense phenomenological consequences. This hypothesis essentially argues that the neutron star "explodes" (i.e., the neutron-star-to-quark-star combustion is explosive). The neutron-rich ejecta released from the outer layers of the exploding neutron star also constitute a very suitable site for nucleosynthesis and r-process elements, since there is a very low proton fraction (Y_e; see Section 3.4).

In the quark-nova investigations, it was found that a very natural way of triggering the detonation of a neutron star is via a "quark core-collapse" where the neutron star core simply collapses into a more compact, *(u,d,s)* configuration, releasing massive amounts of energy. This relies on the crucial coupling between the conversion front (the micro-physics; see [10]) and the dynamics it induces at the scale of the star ($\sim 10^6$ cm; the macro-physics), as discussed in the next section.

2. Quark-Nova: The Macrophysics

The initial setup consist of a cold NS. The conversion from hadronic matter (HM) to *(u,d,s)* is triggered by s-quark seeding in the core [38]. If sufficient s-quarks are seeded into a parcel of quark matter, then the conversion of HM to *(u,d,s)* can proceed unimpeded because s-quarks can behave as catalysts. In the results presented in this review, we chose the Hempel & Schaffner-Bielich (2010; [41]) tabulated EOS to describe the HM layers (overlaying the quark core) because it is well-cited, and, more importantly, its tabular structure is fairly simple and well-documented. The EOS also satisfies the two-solar-mass neutron star constraint. For the *(u,d,s)* EOS, we chose the MIT bag model which consists simply of a Fermi gas with a negative pressure B that confines the gas—the Fermi gas pushes outward but the confinement pressure B pushes inward. In the language of free energy, *(u,d)* acts as an energy barrier between two energy minima, which are the hadronic state (i.e., HM) and the *(u,d,s)* state. Since *(u,d)* exists as a barrier, the hadronic matter will not decay by itself. For some values of B, *(u,d,s)*'s binding energy is lower than for the hadronic matter, while at the same time the binding energy of *(u,d)* is higher than for the hadronic matter. Therefore the absolute stability of *(u,d,s)* can exist while respecting the empirical reality of unstable *(u,d)*. For this work, we have extended the MIT bag EOS to include first-order corrections for the strong coupling constant and included temperature dependencies. Nevertheless, inherent uncertainties to the quark matter EOS we use exist as we assume zero entropy and massless quarks. Moreover, only for certain choices of B does the MIT bag model predict absolutely stable *(u,d,s)* matter. In Figure 1, we compare the free energy per baryon versus temperature for the hadronic EOS of [41], and the *(u,d,s)* matter represented by the MIT bag EOS with strong coupling constant corrections. As can be seen from the figure, the free energy of *(u,d,s)* becomes higher around $T \sim 40$ MeV, which blocks the conversion from hadronic to quark matter. In our simulations, we set an initial temperature of $T = 20$ MeV yielding thermodynamic conditions of a neutron star that will be converted into a proto-quark star (PQS). We tested other hadronic EOSs, but, as stated in our work (see [10] and references therein), the effects of the leptonic weak interaction, including the corresponding weak decay rates and the EOS of electrons and neutrinos, are

at least as important as the uncertainties related to the EOS of HM, *(u,d)* and *(u,d,s)* (see discussion in Section 4.1).

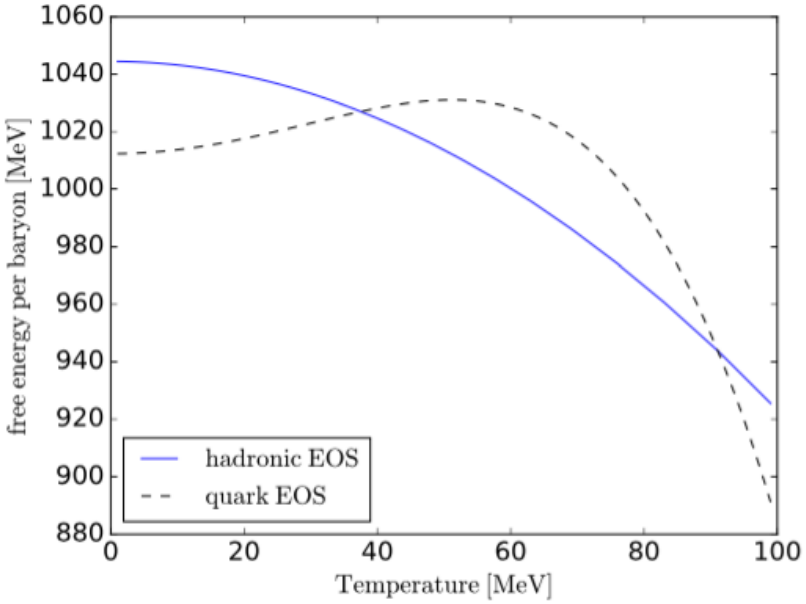

Figure 1. Free energy per baryon versus temperature for the hadronic EOS [41] and that of *(u,d,s)* (the MIT bag EOS with strong coupling constant corrections) used in this work. The free energy of *(u,d,s)* becomes higher around $T \sim 40$ MeV, which blocks the conversion from hadronic to quark matter. Reprinted from Ref. [36].

2.1. The Code

The micro-physics of the quark-nova focuses merely on length-scales of $\sim$0.1 cm to cm (width of the reaction zone) and timescales of about 10^{-8} s (the timescale of the weak interaction that converts d quarks to s quarks). However, in order to study the final fate of a neutron star combusting to a quark star, it is necessary to take into account larger scales.

To truly study this combustion process at a large scale it would be necessary to build a three-dimensional code that combusts the neutron star into a quark star. This code would need to solve the reaction-diffusion-advection equations for the whole star. Such a simulation, although feasible, would be quite difficult to build, since the scales that dominate in the reaction zone (cm) are various orders of magnitude smaller than the scales of the whole compact star (10^6 cm). It would be necessary to use an adaptive computational mesh that uses smaller computational zones for the reaction zone while using larger zones for the rest of the star.

Such a computational code does not exist yet. However, if it is assumed that the burning front remains somewhat well-defined, and therefore instabilities do not distort it significantly, some macroscopic properties of the combustion process can still be derived.

The original attempts to derive the "macroscopic" phenomenology of microphysical studies of the hadron-quark interface hark back to the 1980s, when Olinto et al. wrote their pioneering paper on hadron-quark combustion [30]. In their case, and other similar studies (e.g., [42]), the burning speed was calculated for different densities and then this speed was assumed to be the same for the whole compact star. This approach, even under the assumption that instabilities will not distort the interface too much, or that the boundary conditions of the microphysical problem reflect the macroscopic physics, does not say a great deal about the phenomenology of the conversion, i.e., what the conversion would "look like" through detectors and telescopes. This approach can only be used to calculate a rough timescale for the conversion of the whole neutron star into a quark star, but without calculating the signal detected on Earth.

An interesting imprint that the combustion process leaves behind that should be detectable is a large neutrino signal. Electron neutrinos are produced copiously in quark matter by leptonic processes:

$$u + e^- \rightarrow d + \nu_e \quad (1)$$

$$u + e^- \rightarrow s + \nu_e \quad (2)$$

$$d \rightarrow e^- + \overline{\nu}_e + u \quad (3)$$

$$s \rightarrow e^- + \overline{\nu}_e + u \quad (4)$$

Furthermore, copious τ_ν and μ_ν neutrinos are created through quark breemstralung processes. Neutrinos provide an excellent probe into the combustion process because of their high luminosity and high energies. The reason for the large luminosity is the immense release of energy by the beta equilibration of quark matter. Since the quarks are degenerate, their relaxation into a more stable energy state implies changes of 100 MeV in binding energy. Much of this binding energy is released as neutrinos. Furthermore, the binding energy release is what heats the quark matter, which in turn traps neutrinos and thermalizes them into high temperatures of MeV. Given their energies and luminosities (e.g., peak neutrino luminosities of $>10^{55}$ erg/s), neutrinos may serve as a means of confirming the combustion process.

Furthermore, since the expected luminosities and neutrino temperatures are higher than for other phenomena, such as core-collapse supernovae, the spectrum and photometry of neutrinos for the quark-nova should provide an unambiguous probe to discriminate this phenomenon macroscopically from other explosive astrophysical events.

Finally, neutrinos are also important because they are the most dynamic aspect of the quark star's energy budget. Once combustion burns the star, which would happen over timescales shorter than a second (e.g., [37]), assuming that instabilities do not really distort the interface significantly or quench it, the change in the energy density of the profile becomes a function of neutrino transport, much like the case for proto-neutron stars. At this point, hydrodynamic processes, such as convection, become secondary to the process of neutrino transport. In other words, the evolution of the proto-quark star is defined by the evolution of the neutrino profile, and the hydrodynamics are higher-order effects. Therefore, to detect a "signal" that discriminates this combustion process, it would be essential to examine the evolution of the neutrino profile.

2.2. The Hot Proto-Quark Star

Fortunately, there are approaches to studying the neutrino-driven evolution of a compact star without building a complicated three-dimensional code for the hydrodynamics of the combustion process. There is a class of codes called "stellar evolution" codes originally designed to probe the evolution and luminosities of ordinary stars. They solve, through implicit numerical techniques, the transport equations for heat, and couple these transport processes to the equations for the hydrostatic equilibrium of the star (e.g., [43]). This technique was applied to neutron stars. In the neutron star case, the transport equations deal with the general relativistic transport of neutrinos, and the hydrostatic equations are replaced by the general relativistic version of these equations (the Tolman–Openheimmer–Volkoff (TOV) equations).

The reason why these equations must be solved in the general relativistic case, as opposed to the Newtonian case, is the extreme compactness of neutron stars and quark stars which distort space and time because their radius is close to their Schwarzschild radius: $r_s = 2GM/c^2$ where G is the gravitational constant, M is the mass of the object, and c is the speed of light.

For example, neutrinos look "cooler" and "less energetic" to an observer far away from the compact star because of a gravitational red-shifting of the neutrinos, which decrease their frequency from a frame of reference at infinity.

So, under the following assumptions, we can simulate the evolution of the proto-quark star (PQS):

- *Short combustion timescale*: We must assume that the combustion process is much faster than the neutrino evolution process. The reason we should make such an assumption is that, if the neutrino cooling is much longer, it can be assumed that the temperature profile produced by the combustion process "freezes" and is only affected by neutrino transport. Since, outside the combustion process, all other cooling processes that affect the partitioning of the energy budget are much slower than neutrino transport, the microphysical combustion problem can reasonably be decoupled from the large-scale evolution problem, if we assume that combustion is much faster than neutrino transport.
  This assumption of combustion may be supported by microphysical simulations (e.g., [37]). Numerical simulations show that laminar burning speeds can reach 0.001c–0.1c. Assuming these speeds are sustained in the microscopic case, and that instabilities do not slow down the burning front too much, using these numbers would mean that the neutron star would combust into a quark star in a fraction of a second. This timescale must be smaller than the timescale for cooling/deleptonization. We can make a rough order-of-magnitude estimate of the timescale of deleptonization/cooling through dimensional analysis. For the high temperatures > 20 MeV and high densities of a quark star (a few times nuclear saturation density), the neutrino mean free path is about $\lambda_\nu \sim 1$ cm, much smaller than the radius of the PQS of $R_{\mathrm{PQS}} = 10^6$ cm. Through dimensional analysis, we find the timescale of cooling: $\tau_{\mathrm{cool.}} \sim R_{\mathrm{PQS}}^2/(\lambda_\nu c) \sim 33$ s. Since this cooling timescale is much larger than the estimated combustion timescale, this particular assumption is valid.
- *Hydrostatic equilibrium*: This assumption is justified if the timescales studied in the stellar evolution simulation are longer than the hydrodynamic timescales. This can be tested by looking at the sonic time, which is the time a sound wave takes to cross the whole length that is studied. The reason neutrino cooling needs to be slower than the hydrodynamic processes is that the time-steps of the simulation need to be large enough so that pressure gradients along the star are smoothed out by sound waves. In our case, the length-scale is the radius of the PQS. Because the sound speed of degenerate matter is of the order of the speed of light c, the sonic time will be $\tau_s \sim R_{\mathrm{PQS}}/c \sim 3 \times 10^{-5}$ s. Since the cooling timescale, as calculated above, is of the order of 10 s, we can argue that the neutrino cooling is much slower than the hydrodynamic processes, which justifies the hydrostatic assumption.
- *Neutrino trapping*: Most stellar evolution codes for compact stars assume neutrino trapping to be able to simulate neutrino transport with a simple application of Fick's law. Since we know that the mean free path of neutrinos is about 1 cm, while the radius of the quark star is $R \sim 10$ km, the neutrino trapping assumption is reasonable.
- *β-equilibrium*: We must assume that the quarks in the PQS are in chemical equilibrium at each time-step. This assumption makes it possible not to have to keep track of the time-dependent reaction rates that regulate the chemical composition of quark matter. Since the weak interaction in the context of the conversion of two-flavoured to three-flavoured matter has a timescale of $\sim 10^{-8}$ s, we can effectively assume chemical equilibrium, since the cooling/deleptonization timescale, as calculated above, is ~ 10 s.
- *Thermal equilibrium*: In order to assume thermodynamic variables such as pressure, temperature, and chemical potential, we must assume that the neutrinos are thermalized. By thermalized, we imply that the neutrinos have collided and scattered sufficiently so that they can be considered to be at thermal equilibrium. In much of the Universe, neutrinos are seldom thermalized, since their interaction cross-section is tiny; so, once emitted, they pass through matter mostly unperturbed. However, compact stars, such as quark stars, are the only existing systems in the Universe that emit a spectrum of thermal neutrinos. This is due to the extreme densities and temperatures

of these objects; such thermodynamic conditions enlarge the cross-section of neutrinos to the point that they scatter and collide easily with other particles.

2.3. Thermalized Neutrinos and Heat Transport

The fact that neutrinos are thermalized ($\lambda_\nu << R_{\rm PQS}$) makes the simulation much easier than if the neutrinos were not thermal, since the neutrino's temperature is the same as the quark matter's temperature. In this case, the transport equation for the energy density of neutrinos simply corresponds to one diffusion-like equation per flavour. In contrast, if the neutrinos were not thermalized, one would have to solve the Boltzmann transport equations, which requires a very complicated six-dimensional integral, and therefore requires more computational and programming sophistication/resources.

Following the assumptions above, we can outline the equations that our simulation will solve. First, we must write down the relevant space-time metric of the problem:

$$ds^2 = -e^{2\phi}dt^2 + e^{2\lambda}dr^2 + r^2 d\Omega \tag{5}$$

Here, dt is an infinitesimal element of the coordinate time at infinity. $d\Omega$ is an infinitesimal element of the solid angle, and ϕ and λ are metric functions.

The TOV equations that compute the structure of the compact star, that is, the pressure, radius, and density, will be outlined using the above metric and the assumption of hydrostatic equilibrium. The TOV equations in Lagrangian coordinates are:

$$\frac{dr}{da} = \frac{1}{4\pi r^2 n_B e^{\lambda}} \tag{6}$$

$$\frac{dm}{da} = \frac{\epsilon}{n_B e^{\lambda}} \tag{7}$$

$$\frac{d\phi}{da} = \frac{e^{\lambda}}{4\pi r^4 n_B}(m + 4\pi r^2 P) \tag{8}$$

$$\frac{dP}{da} = -(\epsilon + P)\frac{e^{\lambda}}{4\pi r^4 n_B}(m + 4\pi r^3 P) \tag{9}$$

$$e^{-\lambda} = \sqrt{1 - \frac{2m}{r}} \tag{10}$$

where r stands for the radial coordinates, n_B for number density, P for pressure, a for the number of baryons enclosed by a sphere of radius r, and m is the gravitational mass enclosed by radius r. The reason why we choose Lagrangian coordinates over the more common derivation that uses Eulerian coordinates, and therefore r as the integrated quantity, is that the radius of the compact star is time-dependent. Since the radius is not a conserved quantity, the numerical treatment becomes complicated as a computational grid made of radial coordinates would keep changing spatially. In contrast, the total baryon number of the star is conserved, so a computational grid that discretizes along a baryonic coordinate can be constructed.

The transport equations (for lepton fraction Y_L and energy density ϵ) are the following:

$$\frac{\partial Y_L}{\partial t} + \frac{\partial (e^{\phi} 4\pi r^2 (F_{\nu,e})}{\partial a} = 0 \tag{11}$$

$$\frac{\partial \epsilon}{\partial t} + \frac{\partial (e^{2\phi} 4\pi r^2 (H_{\nu,e} + H_{\nu,\mu}))}{\partial a} = 0 \tag{12}$$

$$F_{\nu,e} = \frac{\lambda_{\nu,e}}{3}\frac{n_\nu}{dr} \tag{13}$$

$$H_{\nu,i} = \frac{\lambda_{\nu,i}}{3}\frac{\epsilon_{\nu_i}}{dr} \tag{14}$$

where $F_{\nu,e}$ is the neutrino number density flux and $H_{\nu,i}$ is the neutrino energy density flux. These equations are simply Fick's law as applied to neutrino number densities (n_ν) and neutrino energy density (ϵ_{ν_i}).

The stellar evolution code requires some initial conditions to be set in order to solve the problem. Three important radial parameters that need to be imposed as initial conditions are the baryonic mass, the lepton fraction and the temperature. The initial values of these parameters must be imposed a priori. A useful observation that enables the derivation of these initial distributions is the fact that neutrino transport is probably much slower than the combustion speed; as calculated above, the timescale of neutrino transport is about $\sim$10 s while the timescale of combustion is at most a fraction of a second. We can therefore make the following assumptions that simplify our calculations considerably:

- *Frozen initial temperature profile*: Since the dominant process of cooling is neutrino emission/transport, we can assume that the initial temperature profile can be interpolated from local microscopic simulations that calculate the temperature for a given initial fuel density. This implies that we can decouple the problem into two sets of microphysical and macrophysical simulations: the former calculates the temperature profile through interpolation of temperature calculations for various initial densities, and the latter solves the global, macroscopic equations of neutrino transport. This decoupling simplifies the calculations considerably.
- *Frozen lepton fraction*: Since the combustion process happens at a much faster timescale than the neutrino transport, we can assume that the initial lepton fraction of the unburned neutron star is equivalent to the initial lepton fraction distribution of the hot quark star that is evolved in the code. Through this assumption, we can directly extract the initial lepton fraction from the EOS of a neutron star.
- *Convergence of combustion temperature at low initial hadronic densities:* Our simulations can only calculate the temperature for initial hadronic densities that are not lower than 0.05 fm^{-3}, since, otherwise, the density gradient would be too large, generating numerical instabilities. However, for lower initial densities, such as those found on the edge of the hadronic star, the temperatures of the ash will converge to a similar temperature of $\sim$20 MeV, as the ash will also converge to the same density, since the large confinement pressure of B forces the ash to have a non-zero density in the order of nuclear saturation. Therefore, even if we do not pursue a simulation, we can calculate the neutrinospheric temperature from the binding energy released through two-flavour to three-flavour quark matter equilibration using an analytical argument. Using a zero entropy MIT bag model, in previous sections, we found that the temperature of a baryon can increase to about $\sim$30 MeV. In the numerical scheme for 0.05 fm^{-3} initial hadronic density, this quantity ends up lower, but of the same magnitude, around $\sim$20 MeV, mostly because of the effect of the s-quark mass, where a finite mass leads to less binding energy release.
  The temperature of a neutrinospheric baryon that is about $\sim$20 MeV will mostly cool through neutrino emission. To ensure that the neutrinospheric temperature will remain high for sufficiently long after the combustion process, in order to assume the same high initial neutrinospheric temperature, it is necessary to calculate the cooling timescale. Assuming neutrinos are not trapped in the neutrinosphere, then the neutrinos of neutrinospheric quark matter will automatically escape the moment they are emitted. We can calculate the timescale of cooling analytically with the following prescription obtained from Iwamoto et al. [44].

$$\tau_{\rm cool} \sim 3153 \text{ s} \times \left(\frac{Y_e}{0.01}\right)^{-1/3} \times \left({T_{f_9}}^{-4} - {T_{i9}}^{-4}\right). \tag{15}$$

  In the above, T_{f_9} and T_{i9} are the neutrinosphere's final and initial temperatures in units of 10^9 K. For an initial temperature of around 20 MeV, how long it will take for the temperature to cool off by 50 percent can be determined, assuming that there is no

combustion to "reheat" the interface. Using the above equation, the time necessary for the neutrinosphere to lose 50 percent of its temperature is about $\tau_{\rm cool}\sim10^{-5}$ s. This timescale is actually a lower bound, as the emissivity is proportional to $Y_e^{1/3}$, and, therefore, the emissivity becomes less intense as the lepton fraction lowers due to deleptonization. In order to assume this neutrinosphere temperature, this timescale must be much longer than the time required for the combustion interface to cross its own width. We can calculate the minimum combustion speed where this approximation is valid through the estimate $v = l/\tau_{\rm cool}$. Assuming the reaction zone width is $l = 0.1$ cm and $\tau\sim10^{-5}$ s, as calculated from Equation (15), we obtain $v = 10^4$ cm/s. As even the slowest burning speeds calculated in the literature (e.g., Olinto et al. [30] indicate a lower limit of 1 km/s), we can assume that the neutrinosphere remains "hot" throughout the combustion process.

The first assumption, that of a "frozen initial temperature distribution", simplifies the problem and calculations. Using these assumptions, we can run the Burn-UD code for different initial hadronic densities to calculate the "frozen" temperatures that will be plugged into a stellar evolution code. We ran the Burn-UD microphysical code for five different initial densities (0.05 fm $^{-3}$, 0.1 fm $^{-3}$, 0.2 fm $^{-3}$, 0.3 fm $^{-3}$, 0.4 fm $^{-3}$). Due to the "frozen lepton fraction" assumption, we can impose a lepton profile extracted from a cold neutron star in beta equilibrium [45], which is generally of the order of $Y_e = 0.1$ or less. We ran the simulations with a timescale of the weak interaction $\sim10^{-8}$ s, which amounts to about 10^5 time-steps. These simulations lead to a two-column table of temperature vs. initial density (Table 1). These temperatures and densities can be easily interpolated into a function of temperature that is a function of initial hadronic density.

Table 1. Final temperatures of *(u,d,s)* ash for different initial hadronic number densities, as calculated by solving the reaction-diffusion-advection equations. Burning speed is also included for each initial hadronic number density. Reprinted from Ref. [36].

n_B [fm^{-3}]	T [MeV]	v/c
0.05	22.9	0.00083
0.1	23.1	0.0016
0.2	23.4	0.0025
0.3	26.4	0.0058
0.4	30.4	0.010

In order to impose this temperature distribution into a stellar evolution macroscopic simulation, we perform the following. We solve the TOV equations for a cold neutron star at temperature $T = 0.1$ MeV. This gives a density profile of the hadronic star. Since we have an interpolated function of temperature vs. hadronic density, we can compute the temperature at each computational zone as a function of the density in the zone. This creates a temperature profile. We maintain the temperature fixed at each baryonic coordinate a (see Equation (6)), and then simply switch the EOS from hadronic to quark matter. We solve the TOV equations again to obtain a new quark star density profile, radius, and gravitational mass, while still maintaining the same temperature profile and the same baryonic mass.

2.4. The Neutrino Spectrum

Now that we have constructed our hot PQS, a simulation based on the above assumptions and equations produces the following behavior behind a nascent, hot quark star: the production of entropy by the combustion process creates a nascent quark star with central temperatures of $T\sim30$ MeV and outer temperatures of about $T\sim20$ MeV. The initial lepton fraction is of the order of $Y_L\sim0.1$ since it corresponds to the same lepton fraction as that of a cold neutron star in beta equilibrium. This nascent quark star also has a neutrino density profile with a very high neutrino chemical potential profile of ~100 MeV, since the quark star's densities are always of the order of nuclear saturation density, with the

density decreasing sharply to zero in a height scale of a femtometer (the length scale of the strong interaction). This very hot object of $T > 20$ MeV will cool off in a period of tens of seconds since the heat will utimately be carried away by neutrinos. There is also a Joule heating effect in the neutrino transport, since the initial chemical potential of neutrinos is high, and some of the chemical potential energy is transformed into heat as the neutrinos escape from the quark star (see [10] for the micro-physics of the combustion).

The main ways in which this stellar evolution differs from proto-neutron stars are the following: First, the initial neutrinosphere will be much hotter for the quark star case. As mentioned previously in this section, the neutrinosphere temperature is ∼20 MeV if calculated numerically. This has tremendous consequences for the spectrum and luminosity, as the neutrino energy will be roughly ∼60 MeV and the luminosity is proportional to T_ν^4, where T_ν is the neutrinospheric temperature.

Since the neutrino spectrum is both harder and more luminous for the PQS than the PNS, the neutrino signal, as detected from Earth, will be different for the PQS and the PNS (Figures 2 and 3). First, the PQS will have a very hard spectrum composed of high temperature $T > 20$ MeV neutrinos, which will produce a very different Fermi–Dirac distribution, and, therefore, detected signal, than the PNS, where neutrinos have a temperature of only T∼5 MeV. This harder spectrum also leads to a higher peak luminosity for the PQS, which is >10^{55} erg/s, a luminosity that cannot be produced by PNSs.

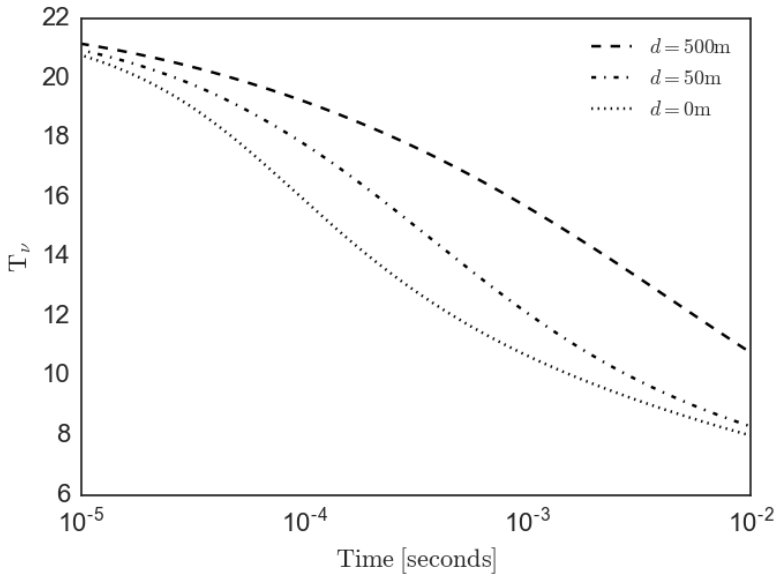

Figure 2. Evolution of the neutrinospheric temperature for the PQS. Each curve represents a different length of the mixed-phase d (in meters). Reprinted from Ref. [36].

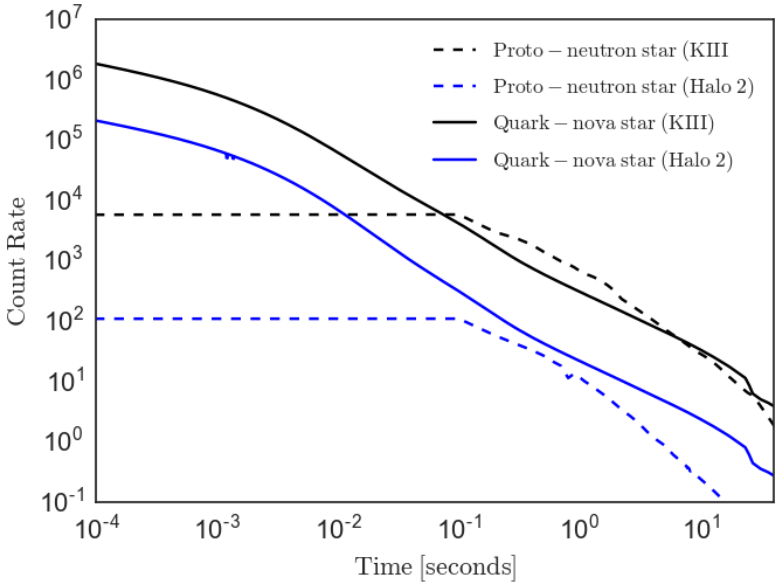

Figure 3. Detector count rates for a quark-nova vs. proto-neutron star for Super-Kamiokande III and Halo 2. Reprinted from Ref. [36].

An interesting question is how would this neutrino signal look in a detector? We will focus in water-based detectors (KIII) and lead-based detectors (Halo 2). In the case of water-based detectors, neutrinos are detected through the emission of secondary positrons by proton absorption of electron anti-neutrinos:

$$\overline{\nu}_e + p \rightarrow e^+ + n. \tag{16}$$

where p, is a proton, n is a neutron, and e^+ is a positron. This cross-section is proportional to E_ν^2, where E_ν is the energy of neutrinos. In the context of Halo II, neutrinos are detected by the emission of neutrons through neutrino capture by lead nuclei:

$$\nu_e + (N, Z) = (N - 1, Z + 1) + e^- + n\,, \tag{17}$$

where (N, Z) is an arbitrary nucleus of N neutrons and Z protons.

Detector counts for the two types of detectors are found in Figure 3. For the first 10^{-2} s, PQS count rates are about two orders of magnitude higher than for the PNS case. Furthermore, the PQS spectrum will be very different, as the neutrinospheric temperatures are much higher for the PQS case, as can be seen from Figure 2. Therefore, we can deduce that the PQS will release a fairly clean signal that should be very different from the case of PNS.

2.5. The Ejecta

Another important aspect is that the large neutrino luminosity of the PQS can potentially transform into kinetic energy through neutrino-antineutrino pair annihilation. This effect arises from the fact that there will be a high density of both neutrinos and antineutrinos, and therefore a high probability of head-on collisions which would annihilate them. The formula for neutrino pair-annihilation is:

$$L_{e^-e^+} = 1.09 \times 10^{-5} \times (D_1\, L_{\nu_e,51}^{9/4} + D_2\, L_{\nu_\mu,51}^{9/4} + D_2\, L_{\nu_\tau,51}^{9/4}) R_{\mathrm{PQS},6}^{-3/2} \tag{18}$$

where $L_{e^-e^+}$ is the energy per second deposited as e^-e^+ pairs and $L_{\nu_i,51}$ is neutrino luminosity in units of 10^{51} erg/s, $D_1 = 1.23$ and $D_2 = 0.814$ [46]; the proto-quark star radius R_{PQS} is in units 10^6 cm.

This implies that annihilation is proportional to T_ν^9, which means this effect is extremely sensitive to temperature. The pair annihilation mechanism has already been explored in the context of core-collapse supernovae and neutron star mergers (e.g., [47]). In the case of supernovae, it was originally conceived as a mechanism that could inject sufficient energy to revive the stalled shock, with Goodman et al. [47] arguing that the pair annihilation mechanism could inject as much as 10^{51} ergs in mechanical energy, which is the same kinetic energy observed in ordinary core-collapse explosions. However Cooperstein et al. [48] found that the original value of 10^{51} ergs was a gross overestimation, since Goodman et al. had overestimated the energy of neutrinos, and had not taken into account the fact that the reverse pair annihilation reaction could annihilate the electron-positron pairs to produce cooling, which sapped the shock from the energy necessary to eject the supernova shell. Therefore, in the case of supernovae, the pair annihilation mechanism contributes negligibly to the explosion.

However, in the case of the PQS, there are differences in the physics of the neutrinosphere from the PNS case that makes the pair annihilation mechanism a powerful explosive engine. First, there is the fact that the neutrinosphere of the PQS is extremely hot, with a temperature of about $T\sim$20 MeV. This high temperature is due to combustion, which heats up the whole star, including the neutrinosphere. This large temperature makes an immense difference in the energy deposited by the pair annihilation mechanism for the PQS in contrast to the PNS. We can calculate the ratio between the two by noting that the pair annihilation mechanism is proportional to T_ν^9. Assuming the neutrinospheric temperature of PNS is $T_{\nu\mathrm{PNS}}\sim$5 MeV, and that for the PQS is $T_{\nu\mathrm{PQS}}\sim$20 MeV, the ratio between the two is:

$$\frac{T_{\nu\mathrm{PQS}}^{\ 4}}{T_{\nu\mathrm{PNS}}^{\ 4}} = 4^9 \sim 3\times 10^5\ . \tag{19}$$

In other words, the energy deposited through pair annihilation in PQS is more than five orders of magnitude larger than for PNS! Furthermore, the PQS does not suffer the same sort of electron-positron annihilation cooling as for the case of the PNS, since in the PQS case, along the interface, there is an extreme temperature drop of 20 MeV with a scale height of less than one centimeter. Since the cross-section for electron-positron annihilation is proportional to temperature, then the cooling rates are of lesser magnitude than the neutrino annihilation heating rates, since the latter have a much larger temperature than the former.

We can estimate how much energy is injected through pair annihilation by using the time-dependent output of the stellar evolution code, since the pair annihilation mechanism ultimately depends on temperature.

Preliminary calculations have found that the kinetic energy deposited by pair annihilation can be as much as $\sim 10^{52}$ ergs, depending on the existence of a strangelet-electron mixed phase at the edge of the star [49]. The larger the mixed phase, the more energy is deposited through pair annihilation, as the luminosity is larger. The neutrino luminosity is larger with larger mixed phases because the mean free path becomes enlarged, since a PQS without a mixed phase is extremely dense, of the order of the nuclear saturation density throughout the whole profile, since the density falls very sharply to zero in a scale height of Fermis.

We can estimate how much matter is ejected by the pair annihilation mechanism. A more precise calculation would require solving the hydrodynamic equations behind the PQS wind. However, we can find an analytic approximation of the hydrodynamic equations that can be used to estimate the mass ejection with the use of the time-dependent output of the stellar evolution code. The equations of mass continuity imply that:

$$\frac{dM}{dt} = 4\pi\rho R^2 v_s\ , \tag{20}$$

where $\frac{dM}{dt}$ is the mass ejected per second, ρ is the mass density, R is the radius, and v_s is the velocity of the wind. We assume the mass ejected is the leftover hadronic mass that hovers above the quark-star. We can assume that pair-annihilation "happens" before the whole quark star is burnt; therefore, there will be a small amount of hadronic matter overlaying the quark star that can be ejected. The same can be said for a mixed phase, where the quark-nuggets that are gravitationally bound to an electron lattice can also be ejected by the pair annihilation.

Furthermore, we must have an energy conservation equation where mass is ejected, only if: (i) the energy injected by pair annihilation is more than the gravitational potential energy of the parcel ejected, and (ii) the energy does not transport away as fast as it is injected. Under these two assumptions, we can write the equation of energy conservation:

$$L - GM\frac{dM}{dt}/R = 4\pi\rho v_s^3 R^2 \,, \tag{21}$$

where v_s is the sound speed, M is the mass of the quark star, and G is the gravitational constant.

As the speed of sound, M and R, and L are given, we can solve the two equations above to obtain a solution for the $\frac{dM}{dt}$. The existence of mass ejection through pair-annihilation implies an explosive mechanism that does not require supersonic detonation or core-collapse—it merely requires that the neutrinosphere is hot enough and that the combustion front is faster than the neutrino transport timescale. These conditions are weaker and easier to achieve than core-collapse of the quark core or detonation to a deflagration transition.

We conclude this section by briefly enumerating the mechanisms that can trigger the ejection of the relativistic ejecta. An important set of mechanisms is what we will refer to as "shock-induced ejection". This implies that, in a compact star, the ongoing conversion of hadronic to quark matter shrinks the core too quickly for the overlaying layers to respond, creating a separation or a gap. Given that this requires supersonic falling speeds, this will create a shock. This scenario is similar to core-collapse supernova, where the core shrinks supersonically, separating the outer layers. In this scenario, a couple of things could happen:

- *Mechanical core bounce*: In the case of supersonic core-collapse, the increasing density in the core would make it stiffer, eventually making the infalling matter bounce back. This mechanism has been used in supernova simulations with quark cores (e.g., [50]).
- *Thermal photon fireball*: The surface of a quark star can achieve very high temperatures of $T\sim$20 MeV. This would generate an intense photon flux that could push the crust towards relativistic speeds. This picture is sustained by the fact that the crust "floats" on top of the quark star, leaving a gap between the quark surface and the crust. The photon flux would then act as a piston that pushes the crust outwards. The other issue that occurs in the case of a transition to CFL, is that neutrino emissivities are shut off, making photons the explosive mechanism [51].
- *Detonation*: it could be that instabilities accelerate the laminar flame into supersonic speeds. This would generate an effect referred to as a deflagration to detonation transition (DDT). This would generate a shock that could eject the outer layers of the compact star.
- *Neutrino-induced ejection*: Originally Keränen et al. [52] calculated the mass ejection that is induced by neutrino deposition. From this perspective, the core shrinks supersonically and at the same time emits neutrinos that are absorbed by the overlaying layers, unbounding them gravitationally. In this case, 10^{51} ergs are deposited into the outer hadronic layers.

Here, we argue that, since the neutrinospheric temperature in a PQS will reach $\sim$20 MeV, there will be copious neutrino-antineutrino pairs. These pairs will annihilate above the neutrinosphere into electron-positron pairs that will become tightly coupled with the overlying hadronic matter. Due to momentum conservation, these neutrinos will

deposit their momentum. Our preliminary calculations show that about $\sim 10^{52}$ ergs can be deposited using this mechanism.

Given that, in the case of an isolated quark-nova, the only remaining hadronic matter will be the overlaying crust, then the ejecta will only contain about $\sim 10^{-5} M_{\odot}$ matter. If we assume that about $\sim 10^{52}$ ergs are injected into that crust, we will obtain a Lorenz factor of about a few hundred. Thus the quark-nova has the potential to convert an important percentage of the NS-to-QS conversion energy to relativistic ejecta with interesting implications for astrophysics, as discussed below.

3. Some Applications to High-Energy Astrophysics

The findings presented above did not take into account the presence of a color superconductive quark matter phase. This would allow the channelling of some of the neutrino energy to a photon fireball (see [51] and references therein) making relativistic quark-nova ejecta an even more likely outcome. The relativistic quark-nova ejecta (see Section 2.5) enable an efficient harnessing of the HM-to-*(u,d,s)* conversion energy, converting it to extreme radiation via shock following collision with the environment. An interesting aspect of the mass ejection mechanism is the possibility that it produces strong electromagnetic signatures with a total energy of 10^{52} ergs. There are two avenues for the production of these signatures. The first avenue is when the quark-nova explodes in isolation; in other words, the quark-deconfinement that produces the mass ejection appears in a fairly old neutron star, where the supernova ejecta of the progenitor explosion has dispersed, giving rise to a neutron star in isolation. The other case is when a neutron star explodes while still embedded within the ejected envelope of its supernova progenitor. Under these two scenarios, the quark-nova model was found to account for the main high-energy astrophysical phenomena and, in particular, those facing the energy budget discussed in the introduction.

3.1. Superluminous SuperNovae (SLSNe)

A dual-shock quark-nova (dsQN) happens when the quark-nova occurs days to weeks after the supernova (SN) explosion of the progenitor star. The time delay means that the quark-nova ejecta catch up and collide with the SN ejecta after it has expanded to large radii [53]. Effectively, the quark-nova re-energizes the extended SN ejecta causing a re-brightening of the SN; most of the ejecta's energy (i.e., $\sim 10^{52}$ ergs) can thus be converted to radiation! For time delays not exceeding a few days, and because of PdV losses, the size of the SN ejecta is small enough that only a modest re-brightening results when the quark-nova ejecta collides with the preceding SN ejecta; this yields a moderately energetic, high-velocity, SN. However, in this case, the quark-nova model predicts that the interaction of the quark-nova neutrons with the SN ejecta leads to unique nuclear spallation products [54]. For longer time delays, extreme re-brightening occurs when the two ejecta collide yielding light curves very similar to those of SLSNe [55]. For time-delays exceeding many weeks, the SN ejecta is too large and too diffuse to experience any substantial re-brightening.

A quark-nova could also occur in tight binaries where the NS can accrete/gain enough mass to increase its core density and experience a quark-nova event. The NS can accrete either from the companion overflowing its Roche lobe [56] or while inside a binary's common envelope. Quark-novae in binaries have proven successful in fitting properties of unusual SNe (see [57] for details). The quark-nova model (applied to buried and isolated NS) has been used to fit a large number of superluminous and double-humped supernovae (see http://www.quarknova.ca/LCGallery.html (accessed on 20 March 2022) for a picture gallery of the fits).

3.2. Gamma-Ray Bursts (GRBs)

For longer delays of years to decades following the core-collapse of a massive star (e.g., a Type Ic SN), Ref. [58] built a model capable of explaining many of the key characteristics of gamma-ray bursts (GRBs). Here, one appeals to the turbulent (i.e., filamentary and magnetically saturated) SN ejecta, shaped by its interaction with an underlying pulsar wind

nebula (PWN), and sprayed by the relativistic quark-nova ejecta. Synchrotron radiation is emitted as the quark-nova ejecta passes through successive filaments explaining the light-curves of many observed GRBs including the flares and the afterglow. We successfully fitted the light-curves in the XRT-band (including the afterglow and the flares when present) simultaneously with the spectrum for each of the many GRBs we selected; see Section 5.3.1 and Figure 6 in [58].

3.3. Fast Radio Bursts (FRBs)

Old, slowly rotating and isolated NSs in the outskirts of galaxies experiencing a quark-nova event can yield fast radio bursts [59]. The quark-nova ejecta expanding in a low-density medium develops plasma instabilities (Buneman and Weibel successively) yielding electron bunching and coherent synchrotron emission with properties of repeating and non-repeating FRBs, such as the GHz frequency, the milli-second duration and a fluence in the Jy ms range. (The reader is encouraged to run the quark-nova FRB simulator at http://www.quarknova.ca/FRBSimulator/ (accessed on 20 March 2022)).

3.4. R-Process Nucleo-Synthesis

The presence of neutron-rich, large Z nuclei in the QN ejecta (i.e., the neutron star's outermost layers with $(40, 95) < (Z, A) < (70, 177)$), the large neutron-to-seed ratio, and the low electron fraction $Y_e \sim 0.03$ in the decompressing ejecta present favorable conditions for rapid neutron capture (r-process) nucleosynthesis. The quark-nova provides a rich supply of exotic nuclei and generates an r-process environment that is similar, though not identical, to neutron star mergers (NSMs). The QN and NSM scenarios both utilize decompression of neutron matter for the r-process, but the underproduction of elements at $A < 130$, known as a feature of NSM yields, is less pronounced in the QN [60,61]. The quark-nova ejecta is a natural rapid neutron-capture (r-process) site [61]. With an estimated quark-nova rate of 0.1 that of core-collapse supernovae and an ejecta of $\sim 10^{-5} M_\odot$ per quark-nova, these could be an important source of r-process elements ejecting $\sim 10^{-8} M_\odot$ per year per galaxy of r-process products. This is of the same order as the contribution from binary mergers which occur at a much lower rate of $\sim 10^{-6} M_\odot$ per year per galaxy but with a much higher ejecta mass of $\sim 10^{-2} M_\odot$ per merger.

There are implications of the quark-nova r-process nucleosynthesis for astrophysics. These include: (i) A neutron star experiencing a quark-nova event while still embedded within the supernova remnant can deposit NSM-like r-process material into the expanding shell; (ii) quark-novae occur naturally within Pop. III stars, thus contributing to the r-enrichment of the interstellar medium much before NSMs which would instead lead to a sudden and late r-enrichment [62]; (iii) The neutron-rich relativistic quark-nova ejecta was shown to be an efficient spallation process converting ^{56}Ni to ^{44}Ti when interacting with the preceding SN ejecta [54]. This novel process of destroying ^{56}Ni would have the unexpected effect of dimming some supernovae (e.g., [63]).

4. Discussion

The work of the Quark-Nova group in simulating the non-premixed hadron-to-quark combustion starting with Niebergal [35] was seminal, since the time-dependent solutions were solved for the first time. These early investigations used neither neutrino transport, nor a hadronic EOS, and the halting solution (of the burning front) was based on hybrid arguments which appeal to semi-analytic and numerical analyses. In subsequent work [36], the Burn-UD code was extended by adding neutrino transport, electron EOS, neutrino EOS, and a hadronic EOS. From these additions, we found, for the first time, that neutrinos do indeed induce mechanical instabilities, since they can quench the burning. Furthermore, the addition of hadronic EOS (i.e., HM-to-*(u,d,s)* combustion compared to the *(u,d)*-to-*(u,d,s)* version) leads to thermodynamic effects that may quench or accelerate burning. A major result is that the neutrino heating experienced by hadronic matter due to absorption of neutrinos produced by the beta equilibrating of *(u,d,s)* ash, will lead to a free-energy barrier

between the *(u,d,s)* ash and the hadronic fuel (see [10] for a recent review). This energy barrier can quench the burning. Specifically, in comparing *(u,d)*-to-*(u,d,s)* versus HM-to-*(u,d,s)* burning, the latter (i.e., the inclusion of a hadronic EOS) can generate non-linear thermodynamic effects where the coupling of neutrino transport and the free energy of the hadronic EOS can lead to quenching. This quenching appears since the hadronic fuel can absorb neutrinos emitted by the hot *(u,d,s)*, which can lead to the erection of a free-energy barrier that makes combustion thermodynamically unfavourable. These results suggest that a multidimensional code is necessary, since instability would lead to a wrinkling of the interface, and, therefore, only through a multidimensional study can we unearth the final fate of the burning neutron star.

4.1. Quark-Novae and the EOS of Dense Matter

We note that the formation and properties (e.g., temperature) of the hot proto-quark star, driven by the pressure gradients that drive the burning interface, are controlled primarily by leptonic weak decays rather than by the EOS of the hadronic matter. Specifically, the effects of the leptonic weak interaction, including the corresponding weak decay rates and the EOS of electrons and neutrinos, are at least as important as the uncertainties related to the EOS of high density matter (see [10,36] for details). In the work presented here, we explored hadronic EOSs with a proton fraction less than 0.1, but, in general, the proton fraction, while important, is not as crucial as the strong pressure gradients induced by leptonic weak decays which drastically slow down the burning speed (by orders of magnitude), which is thereafter controlled by the much slower burning process driven by back-flowing downstream matter. The relativistic mean-field approach used in [41] is not unique and other approaches taking into account nuclear many-body interactions rather than reducing the interactions to mean fields exist [64,65]. We plan to explore other hadronic EOSs, both stiff and soft ones including hyperons.

The MIT bag EOS only includes confinement but does not emulate chiral symmetry breaking (the process that gives hadrons their large masses compared to the quark masses that constitute them). Some chiral models, such as the Nambu–Jona–Lasinio (NJL) model tend to reduce the stability of *(u,d,s)*, since the quarks become massive [66]. It is evident that at least some quark matter EOS would not release as much energy through beta equilibration, and therefore lead to lower temperatures for the *(u,d,s)* ash. We are currently exploring a wider parameterization across different quark matter EOSs.

The observation of an energetic quark-nova (e.g., in re-energized core-collapse SNe or in double-humped SNe; see Section 3.1) would support the suggestion that: (i) The transition was first-order (i.e., release of latent heat during the HM-to-*(u,d,s)* transition); (ii) Interface instabilities (e.g., deleptonization; [34]) would have taken place which would favor HM EOS poor in proton fraction in concert with neutrino trapping; (iii) From the total energy released, one could, in principle, differentiate a deflagration-to-detonation from a (quark) core-collapse scenario; (iv) The time delay between the supernova and the quark-nova (weeks in the case of double-humped SNe; see Section 3.1) could be used to investigate: (iv-a) The density at which quark matter deconfines (which is very uncertain). The time delay is the time it takes the core of the neutron star to reach quark deconfinement density due to either spin-down or accretion; (iv-b) s-quark seeding timescales as the most likely mechanisms.

While constraints on the HM and *(u,d,s)* EOSs could be gleaned from the observation of a quark-nova as described above, better interpretation of the observations depends on exploring more EOSs to understand their exact role in the conversion front compared to pressure gradients (from leptonic weak decays and for different electron EOSs) that drive the burning interface.

4.2. Quark-Novae and Binary Neutron Star Mergers

Section 2.5 discusses the quark-nova ejecta which consists mainly of the NS's outermost layers (i.e., the crust) with $M_{\rm QN}{\sim}10^{-5}M_{\odot}$. With up to 10^{52} ergs of conversion

energy converted to kinetic energy, this means an ejecta with a Lorentz factor of hundreds. In other words, compared to binary mergers and SNe, the quark-nova ejecta, besides being neutron-rich and efficient at r-process nucleo-synthesis (see Section 3.4), is highly relativistic. Numerical simulations of NSMs suggest that the type of merger depends strongly on the total mass of the binaries, the mass ratio and on the HM EOS. Prompt black hole formation would naturally be expected if the EOS is soft, while a stiff EOS would yield a hyper-massive NS (HMNS; e.g., [67–69]). Of relevance to the quark-nova model, is the long-lived (>100 ms) HMNS scenario where the massive NS may undergo a quark-nova transition before a black hole forms. An HMNS is more likely to harbour a quark core; once two-lavoured quark matter is nucleated in the core of the HMNS, the weak interaction can turn some of the d quarks into s-quarks, lowering the Fermi energy of the quark matter. The conversion of the HMNS to a quark star is not unrealistic if it occurs on timescales shorter than the black hole formation. An interesting outcome is a short gamma-ray burst from the interaction of the relativistic quark-nova ejecta with the binary's ejecta (see Section 3.2).

Adding the quark-nova into the NSM picture would help relax the need for a short-duration gamma-ray burst driven by accretion onto the black-hole and would provide a new channel for gravitational wave (GW) signals (see Section 4.3). The GWs would be emitted in the time frame between the formation of the HMNS and the collapse to a black hole. Our model would thus predict a short-duration gamma-ray burst prior to black hole formation but following the quark-nova GW signal. The NSM ejecta ($\sim 10^{-2} M_{\odot}$) dwarfs the QN ejecta ($\sim 10^{-5} M_{\odot}$). Nevertheless, the relativistic nature of the QN ejecta plausibly implies the presence of unique exotic nuclei at $A < 130$ not expected from NSMs (see Section 3.4).

4.3. Quark-Novae and Gravitational Waves

Preliminary investigation of gravitational waves from a quark-nova used Newtonian gravity (see Appendix in [70]). The ultimate goal is to compute the GW signal during the HM-to-*(u,d,s)* burning (i.e., during the outward expansion of the hadronic-to-quark matter conversion front) using a full general relativistic treatment which is currently being pursued by the Quark-Nova group. The extreme densities in the burning NS core and instabilities unique to the HM-to-*(u,d,s)* burning (e.g., the deleptonization) should favour specific modes. Ultimately, we hope to isolate unique features of quark-nova GWs to differentiate them from supernovae and binary mergers.

5. Conclusions

By coupling a stellar evolution code to the Burn-UD code, we studied the formation and evolution of a hot proto-quark star (the macro-physics of the quark-nova). We found much higher peak neutrino luminosities (>10^{55} erg/s) and a harder neutrino spectrum than previous stellar evolution studies on proto-quark stars (e.g., Pagliara et al. (2013)). The neutrino counts derived were those that observatories such as Super-Kamiokande-III and Halo-II should expect and could be used to differentiate between a supernova and a quark-nova. Due to the high peak neutrino luminosities in a quark-nova, neutrino pair annihilation can deposit as much as 10^{52} ergs in kinetic energy in the matter overlaying the neutrinosphere, yielding a relativistic ejecta. The energetics of the quark-nova and the dynamics of its ejecta have interesting implications for high-energy astrophysics and could aid in our understanding of many still enigmatic astrophysical transients, such as super-luminous supernovae, gamma-ray bursts and fast radio bursts.

Funding: This research is funded by the Natural Sciences and Engineering Research Council of Canada.

Conflicts of Interest: The authors declare no conflict of interest.

References

1. Janka, H.-T.; Melson, T.; Summa, A. Physics of core-collapse supernovae in three dimensions: A sneak preview. *Annu. Rev. Nucl. Part. Sci.* **2016**, *66*, 341–375. [CrossRef]
2. Kumar, P.; Zhang, B. The physics of gamma-ray bursts and relativistic jets. *Phys. Rep.* **2015**, *561*, 1–109. [CrossRef]
3. Abbott, B.; Abbott, R.; Abbott, T.; Acernese, F.; Ackley, K.; Adams, C.; Adams, T.; Addesso, P.; Adhikari, R.; Adya, V.; et al. Gravitational waves and gamma-rays from a binary neutron star merger: GW170817 and GRB 170817A. *Astrophys. J. Lett.* **2017**, *848*, L13. [CrossRef]
4. Sukhbold, T.; Woosley, S. The most luminous supernovae. *Astrophys. J. Lett.* **2016**, *820*, L38. [CrossRef]
5. Ouyed, R.; Dey, J.; Dey, M. Quark-Nova. *Astron. Astrophys.* **2002**, *390*, L39–L42. [CrossRef]
6. Bodmer, A. Collapsed nuclei. *Phys. Rev. D* **1971**, *4*, 1601. [CrossRef]
7. Terazawa, H. *Tokyo University Report INS336*; Tokyo University: Tokyo, Japan, 1979.
8. Witten, E. Cosmic separation of phases. *Phys. Rev. D* **1984**, *30*, 272. [CrossRef]
9. Weber, F. Strange quark matter and compact stars. *Prog. Part. Nucl. Phys.* **2005**, *54*, 193–288. [CrossRef]
10. Ouyed, R. The micro-physics of the Quark-Nova: Recent developments. In *Exploring the Astrophysics of the XXI Century with Compact Stars*; World Scientific Publishing: Singapore, 2022; ISBN 978-981-122-093-7.
11. Glendenning, N.K. First-order phase transitions with more than one conserved charge: Consequences for neutron stars. *Phys. Rev. D* **1992**, *46*, 1274. [CrossRef]
12. Alford, M.G.; Rajagopal, K.; Reddy, S.; Wilczek, F. Minimal color-flavor-locked–nuclear interface. *Phys. Rev. D* **2001**, *64*, 074017. [CrossRef]
13. Lugones, G.; Grunfeld, A.G.; Ajmi, M.A. Surface tension and curvature energy of quark matter in the Nambu–Jona-Lasinio model. *Phys. Rev. C* **2013**, *88*, 045803. [CrossRef]
14. Paschalidis, V.; Yagi, K.; Alvarez-Castillo, D.; Blaschke, D.B.; Sedrakian, A. Implications from GW170817 and I-Love-Q relations for relativistic hybrid stars. *Phys. Rev. D* **2018**, *97*, 084038. [CrossRef]
15. Alvarez-Castillo, D.E.; Blaschke, D.B.; Grunfeld, A.G.; Pagura, V.P. Third family of compact stars within a nonlocal chiral quark model equation of state. *Phys. Rev. D* **2019**, *99*, 063010. [CrossRef]
16. Bhattacharyya, A.; Mishustin, I.N.; Greiner, W. Deconfinement phase transition in compact stars: Maxwell versus Gibbs construction of the mixed phase. *J. Phys. G Nucl. Phys.* **2010**, *37*, 025201. [CrossRef]
17. Yasutake, N.; Lastowiecki, R.; Benic, S.; Blaschke, D.; Maruyama, T.; Tatsumi, T. Finite-size effects at the hadron-quark transition and heavy hybrid stars. *Phys. Rev. C* **2014**, *89*, 065803. [CrossRef]
18. Alford, M.G.; Han, S. Characteristics of hybrid compact stars with a sharp hadron-quark interface. *Eur. Phys. J. A* **2016**, *52*, 62. [CrossRef]
19. Glendenning, N.K. Phase transitions and crystalline structures in neutron star cores. *Phys. Rept.* **2001**, *342*, 393. [CrossRef]
20. Carroll, J.D.; Leinweber, D.B.; Williams, A.G.; Thomas, A.W. Phase transition from quark-meson coupling hyperonic matter to deconfined quark matter. *Phys. Rev. C* **2009**, *79*, 045810. [CrossRef]
21. Weissenborn, S.; Sagert, I.; Pagliara, G.; Hempel, M.; Schaffner-Bielich, J. Quark matter in massive compact stars. *Astrophys. J.* **2011**, *740*, L14. [CrossRef]
22. Fischer, T.; Sagert, I.; Pagliara, G.; Hempel, M.; Schaffner-Bielich, J.; Rauscher, T.; Liebendörfer, M. Core-collapse supernova explosions triggered by a quark–hadron phase transition during the early post-bounce phase. *Astrophys. J. Suppl.* **2011**, *194*, 39. [CrossRef]
23. Schulze, H.-J.; Rijken, T. Maximum mass of hyperon stars with the Nijmegen ESC08 model. *Phys. Rev. C* **2011**, *84*, 035801. [CrossRef]
24. Maruyama, T.; Chiba, S.; Schulze, H.-J.; Tatsumi, T. Hadron-quark mixed phase in hyperon stars. *Phys. Rev. D* **2007**, *76*, 123015. [CrossRef]
25. Masuda, K.; Hatsuda, T.; Takatsuka, T. Hadron–quark cross-over and massive hybrid stars. *Prog. Theor. Exp. Phys.* **2013**, *7*, 073.
26. Alvarez-Castillo, D.; Blaschke, D.; Typel, S. Mixed phase within the multi-polytrope approach to high-mass twins. *Astron. Nachr.* **2017**, *338*, 1048. [CrossRef]
27. Dexheimer, V.; Negreiros, R.; Schramm, S. Role of strangeness in hybrid stars and possible observables. *Phys. Rev. C* **2015**, *91*, 055808. [CrossRef]
28. McLerran, L.; Reddy, S. Quarkyonic Matter and Neutron Stars. *Phys. Rev. Lett.* **2019**, *122*, 122701. [CrossRef]
29. Prakash, M.; Bombaci, I.; Prakash, M.; Ellis, P.J.; Lattimer, J.M.; Knorren, R. Composition and structure of proto-neutron stars. *Phys. Rept.* **1997**, *280*, 1. [CrossRef]
30. Olinto, A.V. On the conversion of neutron stars into strange stars. *Phys. Lett. B* **1987**, *192*, 71–75. [CrossRef]
31. Perez-Garcia, M.A.; Silk, J.; Stone, J.R. Dark matter, neutron stars, and strange quark matter. *Phys. Rev. Lett.* **2010**, *105*, 141101. [CrossRef]
32. Benvenuto, O.; Horvath, J. Evidence for strange matter in super-novae? *Phys. Rev. Lett.* **1989**, *63*, 716. [CrossRef]
33. Drago, A.; Lavagno, A.; Parenti, I. Burning of a hadronic star into a quark or a hybrid star. *Astrophys. J.* **2007**, *659*, 1519. [CrossRef]
34. Ouyed, R.; Niebergal, B.; Jaikumar, P. Explosive Combustion of a Neutron Star into a Quark Star: The non-premixed scenario. In Proceedings of the Compact Stars in the QCD Phase Diagram III (CSQCD III), Guarujá, Brazil, 12–15 December 2012.

35. Niebergal, B. Hadronic-to-Quark-Matter Phase Transition: Astrophysical Implications. Ph.D. Thesis, University of Calgary, Calgary, AB, Canada, 2011; Publication Number: AAT NR81856.
36. Ouyed, A. The Neutrino Sector in Hadron-Quark Combustion: Physical and Astrophysical Implications. Ph.D. Thesis, University of Calgary, Calgary, AB, Canada, 2018.
37. Niebergal, B.; Ouyed, R.; Jaikumar, P. Numerical simulation of the hydrodynamical combustion to strange quark matter. *Phys. Rev. C* **2010**, *82*, 062801. [CrossRef]
38. Ouyed, A.; Ouyed, R.; Jaikumar, P. Numerical simulation of the hydrodynamical combustion to strange quark matter in the trapped neutrino regime. *Phys. Lett. B* **2018**, *777*, 184–190. [CrossRef]
39. Lugones, G. From quark drops to quark stars. *Eur. Phys. J. A* **2016**, *52*, 53. [CrossRef]
40. Drago, A.; Pagliara, G. The scenario of two families of compact stars. *Eur. Phys. J. A* **2016**, *52*, 41. [CrossRef]
41. Hempel, M.; Schaffner-Bielich, J. A statistical model for a complete supernova equation of state. *Nucl. Phys. A* **2010**, *837*, 210–254. [CrossRef]
42. Furusawa, S.; Sanada, T.; Yamada, S. Hydrodynamical study on the conversion of hadronic matter to quark matter: I. shock-induced conversion. *Phys. Rev. D* **2016**, *93*, 043018. [CrossRef]
43. Pons, J.A.; Steiner, A.W.; Prakash, M.; Lattimer, J.M. Evolution of proto-neutron stars with quarks. *Phys. Rev. Lett.* **2001**, *86*, 5223. [CrossRef]
44. Iwamoto, N. Neutrino emissivities and mean free paths of degenerate quark matter. *Ann. Phys.* **1982**, *141*, 1–49. [CrossRef]
45. Gao, Z.-F.; Shan, H.; Wang, W.; Wang, N. Reinvestigation of the electron fraction and electron fermi energy of neutron star. *Astron. Nachrichten* **2017**, *338*, 1066–1072. [CrossRef]
46. Salmonson, J.D.; Wilson, J.R. Neutrino annihilation between binary neutron stars. *Astrophys. J.* **2001**, *561*, 950. [CrossRef]
47. Goodman, J.; Dar, A.; Nussinov, S. Neutrino annihilation in type ii supernovae. *Astrophys. J.* **1987**, *314*, L7–L10. [CrossRef]
48. Cooperstein, J.; Horn, L.V.D.; Baron, E. Neutrino pair energy deposition in supernovae. *Astrophys. J.* **1987**, *321*, L129–L132. [CrossRef]
49. Jaikumar, P.; Reddy, S.; Steiner, A.W. Strange star surface: A crust with nuggets. *Phys. Rev. Lett.* **2006**, *96*, 041101. [CrossRef]
50. Gentile, N.; Aufderheide, M.; Mathews, G.; Swesty, F.; Fuller, G. The QCD phase transition and supernova core collapse. *Astrophys. J.* **1993**, *414*, 701–711. [CrossRef]
51. Ouyed, R.; Rapp, R.; Vogt, C. Fireballs from quark stars in the color-flavor locked phase: Application to gamma-ray bursts. *Astrophys. J.* **2005**, *632*, 1001. [CrossRef]
52. Keränen, P.; Ouyed, R.; Jaikumar, P. Neutrino emission and mass ejection in Quark-Novae. *Astrophys. J.* **2005**, *618*, 485. [CrossRef]
53. Ouyed, R.; Leahy, D. Dynamical and thermal evolution of the Quark-Nova ejecta. *Astrophys. J.* **2009**, *696*, 562. [CrossRef]
54. Ouyed, R.; Leahy, D.; Ouyed, A.; Jaikumar, P. Spallation Model for the Titanium-Rich Supernova Remnant Cassiopeia A. *Phys. Rev. Lett.* **2011**, *107*, 151103. [CrossRef]
55. Ouyed, R.; Kostka, M.; Koning, N.; Leahy, D.A.; Steffen, W. Quark nova imprint in the extreme supernova explosion SN 2006gy. *MNRAS* **2012**, *423*, 1652. [CrossRef]
56. Ouyed, R.; Staff, J.E. Quark-novae in neutron star—White dwarf binaries: A model for luminous (spin-down powered) sub-Chandrasekhar-mass Type Ia supernovae? *Res. Astron. Astrophys.* **2013**, *13*, 435. [CrossRef]
57. Ouyed, R.; Leahy, D.; Koning, N. Quark-Novae in massive binaries: A model for double-humped, hydrogen-poor, superluminous Supernovae. *Mon. Not. R. Astron. Soc.* **2015**, *454*, 2353–2359. [CrossRef]
58. Ouyed, R.; Leahy, D.; Koning, N. A Quark-Nova in the wake of a core-collapse supernova: A unifying model for long duration gamma-ray bursts and fast radio bursts. *Res. Astron. Astrophys.* **2020**, *20*, 27. [CrossRef]
59. Ouyed, R.; Leahy, D.; Koning, N. Quark-Novae in the outskirts of galaxies: An explanation of the fast radio burst phenomenon. *Mon. Not. R. Astron. Soc.* **2021**, *500*, 4414–4421. [CrossRef]
60. Jaikumar, P.; Meyer, B.S.; Otsuki, K.; Ouyed, R. Nucleosynthesis in neutron-rich ejecta from quark-novae. *A&A* **2007**, *471*, 227–236.
61. Kostka, M. Investigating astrophysical r-process sites: Code (r-Java 2.0) and model (dual-shock Quark-Nova) development. Ph.D. Thesis, University of Calgary, Calgary, AB, Canada, 2014.
62. Ouyed, R.; Pudritz, R.E.; Jaikumar, P. Quark-Novae, cosmic reionization, and early r-process element production. *Astrophys. J.* **2009**, *702*, 1575–1583. [CrossRef]
63. Ouyed, R.; Leahy, D.; Koning, N. Hints of a second explosion (a quark nova) in Cassiopeia A Supernova. *Res. Astron. Astrophys.* **2015**, *15*, 483. [CrossRef]
64. Weber, F.; Weigel, M. Neutron star properties and the relativistic nuclear equation of state of many-baryon matter. *Nucl. Phys. A* **1989**, *493*, 549–582. [CrossRef]
65. Camelio, G.; Lovato, A.; Gualtieri, L.; Benhar, O.; Pons, J.A.; Ferrari, V. Evolution of a proto-neutron star with a nuclear many-body equation of state: Neutrino luminosity and gravitational wave frequencies. *Phys. Rev. D* **2017**, *96*, 043015. [CrossRef]
66. Buballa, M. NJL-model analysis of dense quark matter. *Phys. Rep.* **2005**, *407*, 205–376. [CrossRef]
67. Shibata, M.; Taniguchi, K.; Uryu, K.K. Merger of binary neutron stars with realistic equations of state in full general relativity. *Phys. Rev. D* **2005**, *71*, 084021. [CrossRef]
68. Hotokezaka, K.; Kyutoku, K.; Okawa, H.; Shibata, M.; Kiuc, K. Binary Neutron Star Mergers: Dependence on the Nuclear Equation of State. *Phys. Rev. D* **2011**, *83*, 124008. [CrossRef]

69. Drago, A.; Pagliara, G.; Popov, S.B.The Merger of Two Compact Stars: A Tool for Dense Matter Nuclear Physics. *Universe* **2018**, *4*, 50. [CrossRef]
70. Staff, J.E.; Jaikumar, P.; Chan, V.; Ouyed, R. Spindown of Isolated Neutron Stars: Gravitational Waves or Magnetic Braking? *Astrophys. J.* **2012**, *751*, 24. [CrossRef]